EUROfusion

JET isotope studies and the L-H transition

Emilia R. Solano, JET L2H Team Emilia.Solano@ciemat.es
Laboratorio Nacional de Fusión, CIEMAT, Spain

Special thanks: C. Silva, G. Birkenmeier, E. Delabie

Work supported in part by Spanish National Plan for Scientific and Technical Research and Innovation 2017-2020, grant numbers FIS2017-85252-R and PID2021-127727OB-I00, funded by MCIN/AEI/10.13039/501100011033 and ERDF ‘A way of making Europe’.

MINISTERIO
DE CIENCIA, INNOVACIÓN
Y UNIVERSIDADES

Ciemat
Centro de Investigaciones Energéticas, Medioambientales y Tecnológicas

Laboratorio
Nacional
de Fusión
Ciemat

This work has been carried out within the framework of the EUROfusion Consortium, funded by the European Union via the Euratom Research and Training Programme (Grant Agreement No 101052200 — EUROfusion). Views and opinions expressed are however those of the author(s) only and do not necessarily reflect those of the European Union or the European Commission. Neither the European Union nor the European Commission can be held responsible for them.

JET

The JET L-H transition team

E.R. Solano[1], E. Delabie[2], G. Birkenmeier[3,4], C. Silva[5], J. Hillesheim[6], P. Vincenzi[7], A.H. Nielsen[8], J.J. Rasmussen[8], A. Baciero[1], S. Aleiferis[6,9], I. Balboa[6], A. Boboc[6], C. Bourdelle[10], I.S. Carvalho[5], P. Carvalho[5], M. Chernyshova[11], R. Coelho[5], T. Craciunescu[12], R. Dumont[10], E. de la Luna[1], J. Flanagan[6], M. Fontana[13], J.M. Fontdecaba[1], L. Frassinetti[14], D. Gallart[15], J. Garcia[10], E. Giovannozzi[16], C. Giroud[6], W .Gromelski[11], R. Henriques[5], L. Horvath[6], I. Jepu[12], A. Kappatou[4], D.L. Keeling[6], D. King[6], E. Kowalska-Strzęciwilk[11], M. Lennholm[17], E.L erche[18], E. Litherland-Smith[6], V. Kiptily[6], K. Kirov[6], A. Loarte[19], B. Lomanowski[20], C.F. Maggi[6], M.J. Mantsinen[21], A. Manzanares[22], M. Maslov[6], A.G. Meigs[6], R.B. Morales[6], D. Nina[5], C. Noble[6], V. Parail[6], F. Parra Diaz[23], E. Pawelec[24], G. Pucella[16], D. Réfy[25], E. Righi-Steele[17], F.G. Rimini[6], T.R obinson[6], S. Saarelma[6],M. Sertoli[6], A. Shaw[6], S. Silburn[6], P. Sirén[6], Z. Stancar[26], H. Sun[6], G. Szepesi[6], D. Taylor[6], E. Tholerus[14], S. Vartanian[10], G. Verdoolaege[27], B. Viola[16], H. Weisen[13], T. Wilson[6] and JET Contributors**

EUROfusion Consortium, JET, Culham Science Centre, Abingdon, OX14 3DB, UK

[1]Laboratorio Nacional de Fusión, CIEMAT, Madrid, Spain; [2]Oak Ridge National Laboratory, Oak Ridge, United States of America; [3]Physik-Department E28, Technische Universität München, Garching, Germany; [4]Max-Planck-Institut für Plasmaphysik, Garching, Germany; [5]Instituto de Plasmas e Fusão Nuclear, Instituto Superior Técnico, Universidade de Lisboa, Portugal; [6]CCFE, Culham Science Centre, Abingdon, United Kingdom of Great Britain and Northern Ireland; [7]Consorzio RFX, Padova, Italy; [8]Department of Physics, Technical University of Denmark, Kgs Lyngby, Denmark; [9]NCSR 'Demokritos' 153 10, Agia Paraskevi Attikis, Greece; [10]CEA, IRFM, Saint Paul Lez Durance, France; [11]Institute of Plasma Physics and Laser Microfusion, Warsaw, Poland; [12]The National Institute for Laser, Plasma and Radiation Physics, Magurele-Bucharest, Romania; [13]Ecole Polytechnique Fédérale de Lausanne (EPFL), Lausanne, Switzerland; [14]Fusion Plasma Physics, Stockholm, Sweden; [15]Barcelona Supercomputing Center, Barcelona, Spain; [16]Unità Tecnica Fusione, ENEA C. R. Frascati, Frascati (Roma), Italy; [17]European Commission, B-1049 Brussels, Belgium; [18]Laboratory for Plasma Physics Koninklijke Militaire School, Ecole Royale Militaire Renaissancelaan, Brussels, Belgium; [19]ITER Organization, Saint Paul Lez Durance, France; [20]Aalto University, Aalto, Finland; [21]ICREA and Barcelona Supercomputing Center, Barcelona, Spain; [22]Universidad Complutense de Madrid, Madrid, Spain; [23]Rudolf Peierls Centre for Theoretical Physics, University of Oxford, Oxford, United Kingdom of Great Britain and Northern Ireland; [24]Institute of Physics, Opole University, Opole, Poland; [25]Wigner Research Centre for Physics, Budapest, Hungary; [26]Slovenian Fusion Association (SFA), Jozef Stefan Institute, Ljubljana, Slovenia; [27]Department of Applied Physics, UG (Ghent University), Ghent, Belgium

Acknowledgements: T. Estrada, C. Hidalgo, A. Alonso, D. Carralero, B. van Milligen

*** See the author list of 'Overview of JET results for optimising ITER operation' by J. Mailloux et al to be published in Nuclear Fusion Special issue: Overview and Summary Papers from the 28th Fusion Energy Conference (Nice, France, 10-15 May 2021)*

Outline

- Famous L-H transition movie from MAST
- Fusion, DT, JET
- L-H power threshold. P_{LH}
- P_{LH} scaling
- L-H time evolution, pedestal formation
- Minimum P_{LH} at $n_{e,min}$: isotope effect & critical profiles, A_{eff}
- ExB model vs. measurements: no evolution of v_{perp} along power ramp
- Alternate model: plasma magnetisation, motion of magnetised flux tubes

MAST Video of L-H transition

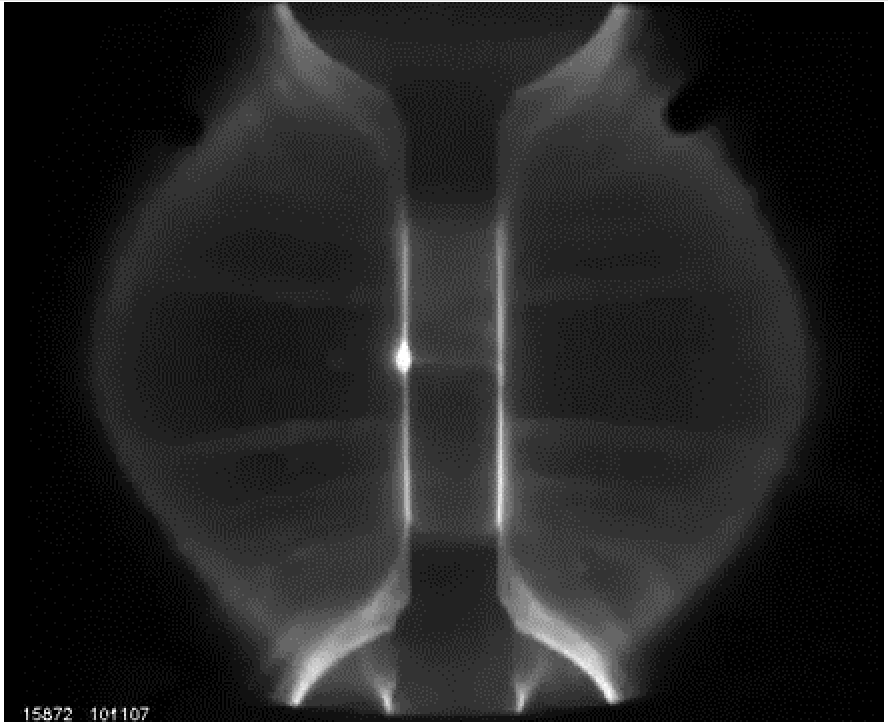

10μs exposure time
1 frame every 0.13 ms
(7.5 kHz)

A Kirk & MAST Team, Plasma Phys. Control. Fusion **48** (2006) B433–B441

What do we see?

- Turbulence at the plasma edge disappears

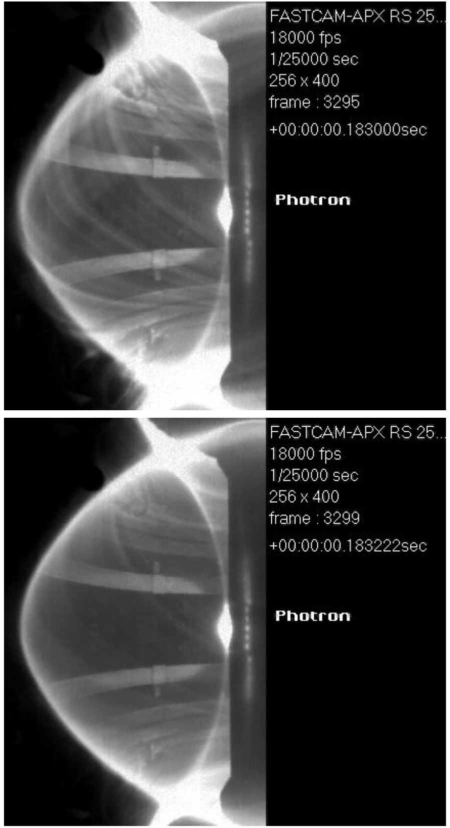

L-mode: the edge looks diffuse, there are spinning plasma filaments that drift outside the separatrix, leading to losses

In ~100 µs. 1-2 frames:

L-H transition

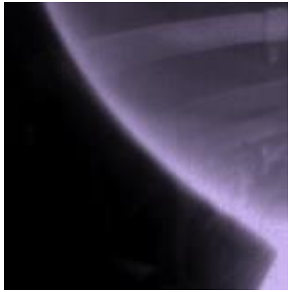

H mode: the edge is sharp, no filaments or turbulence reach accross the separatrix

Fusion

Confinement:

$$\tau_E = \frac{W_{plasma}}{P_{heat}} = \frac{\text{Plasma energy}}{\text{Input power}}$$

Isotopes of Hydrogen

Isotopes, Mix	A, A_{eff}	Plasma confinement	Wall interaction
Hydrogen	1 ●	Poor	Low
Deuterium	2 ■	Medium	Medium
DT 50/50	2.5 ★	Good	Acceptable?
Tritium	3 ◆	Very good	Not always

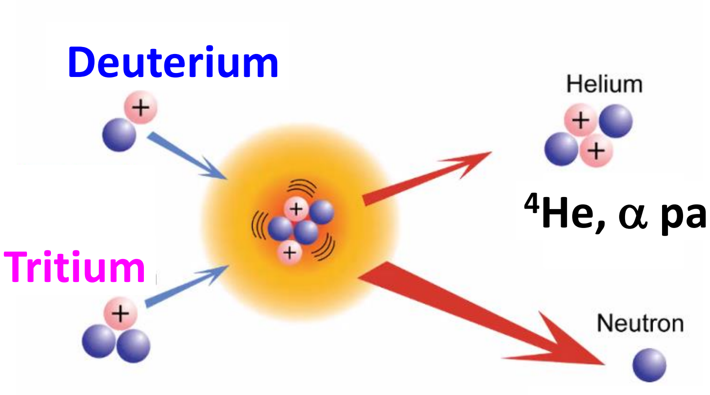

Deuterium

Tritium

^{4}He, α particle 3.5 MeV

Neutron 14 MeV

Ideally T_{ion}>10 kV for optimal DT fusion cross-section

The JET tokamak: Hydrogen, Deuterium, Tritium, DT plasmas

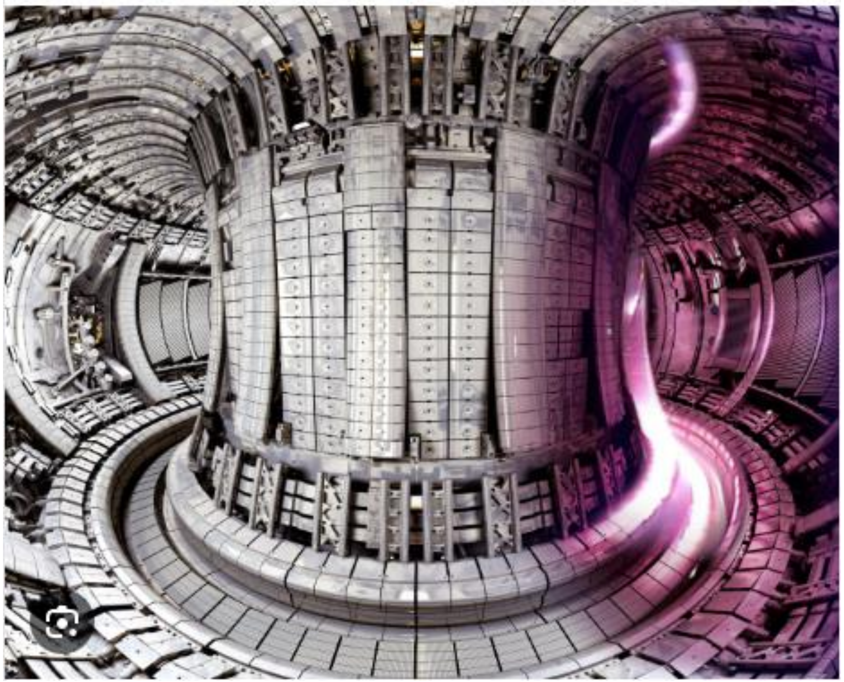

JET-ILW: W divertor, Be walls

Vacuum vessel 4.6 m high x 9 m wide

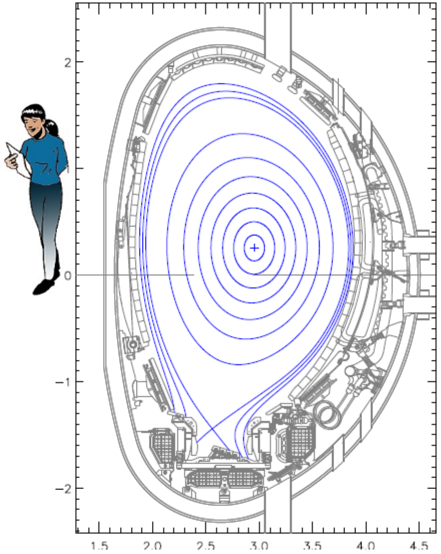

JET Tokamak

Plasma chacteristics:

R= 3 m, a= 1 m

Volume= 80 m^3

I_p≤ 4 MA

B_{tor}≤ 4 T

JET is large!

Unique Tritium and Deuterium-Tritium capability

Stopped end 2023, breaking fusion records

Could be re-started if funding found

Power threshold to reach H-mode

- Discovery of H-mode: F. Wagner Phys. Rev. Lett. 49, 1408 (1982)
- Experiments show that, for otherwise fixed plasma conditions, there is a power threshold to enter H-mode.
- Predicting the appearance of H-mode for future devices requires understanding the power threshold
- In the absence of understanding for L-H transition trigger conditions, experiments with slow power ramps provide measurements of P_{LH}
- Multi-machine scaling studies are used to investigate dependencies of the power threshold.
- Plasma composition affects the power threshold
- Tokamak size, field, current, plasma shape: all affect P_{LH}

Multi-machine P_{LH} databases, scaling

The power required to achieve L-H is measured as:

$$P_{loss} = P_{Ohm} + P_{aux} - dW/dt - PFa_{stLoss}$$

Depending on circumstances and data availability it may be useful to discount bulk radiated power ($\Psi_N<0.95$)

$$P_{sep} = P_{loss} - P_{rad,bulk}$$

ITPA 2008 P_{LH} multimachine scaling, derived for Deuterium, single null, no ECRH heating (quite old).

Martin J. Phys. Conf. Ser. 123 012033 (2008)

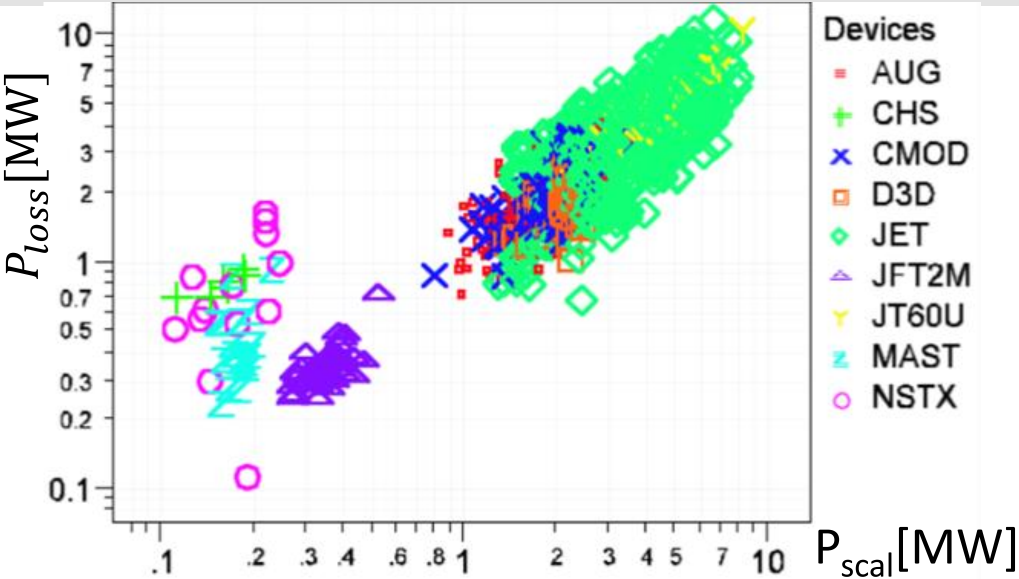

$$P_{scaling} = 0.049\, n_{e20}^{\mathbf{0.72\pm0.03}}\, B_T^{0.83\pm0.03}\, S^{0.94\pm0.02}(2/A)$$

- S is plasma surface area
- n_{e20} average electron density
- n_e, I_p and B_t are colinear in most studies
- **A** represents effective ion mass

Multi-machine P_{LH} databases, scaling

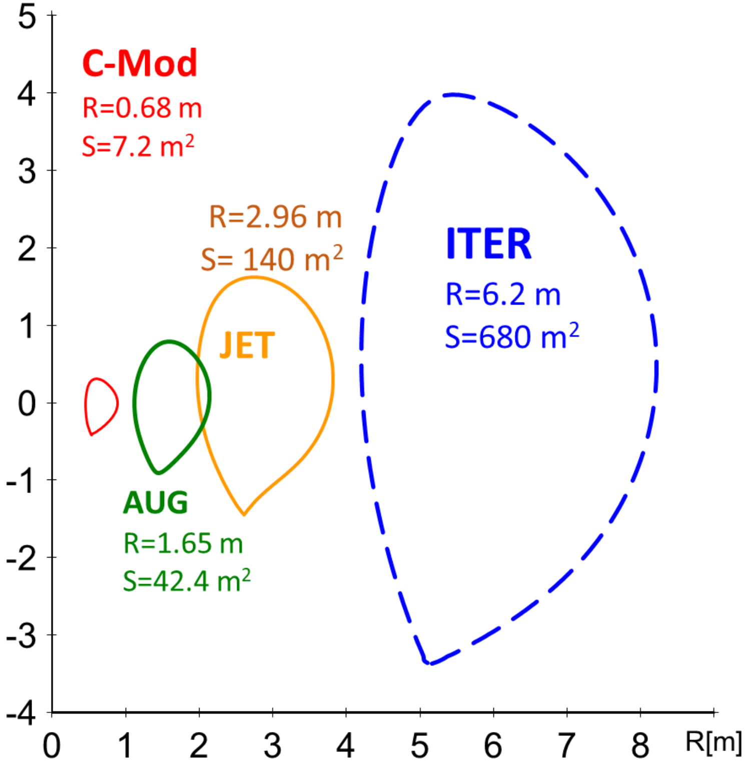

Metal wall makes a difference

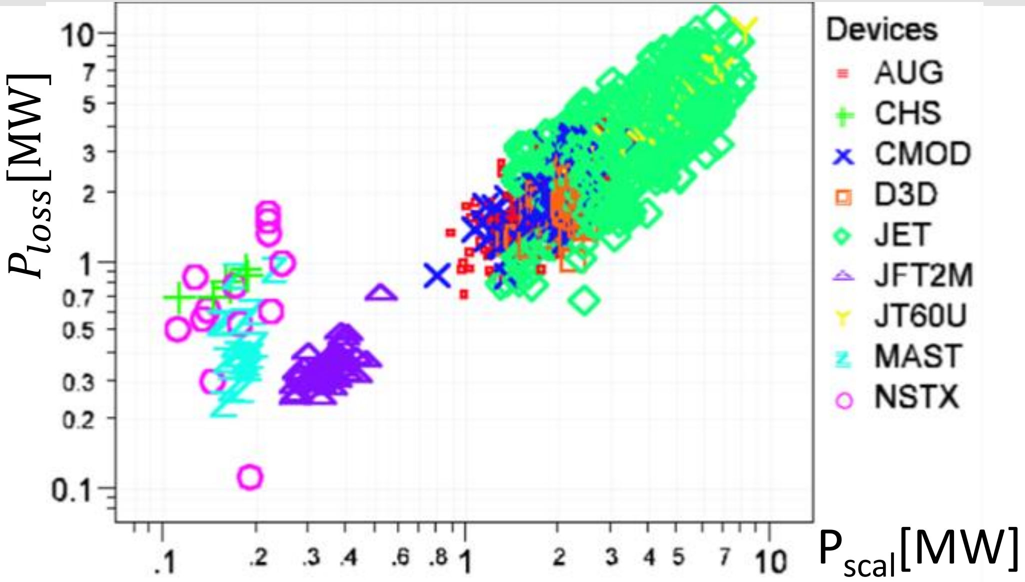

$$P_{scaling}=0.049\, n_{e20}^{\mathbf{0.72\pm0.03}}\, B_T^{0.83\pm0.03}\, S^{0.94\pm0.02}(2/A)$$

Work in progress: metal wall multi/machine scaling, Including new data from AUG, **JET,** C-Mod

L-H transition: from Low to High confinement (H-mode)

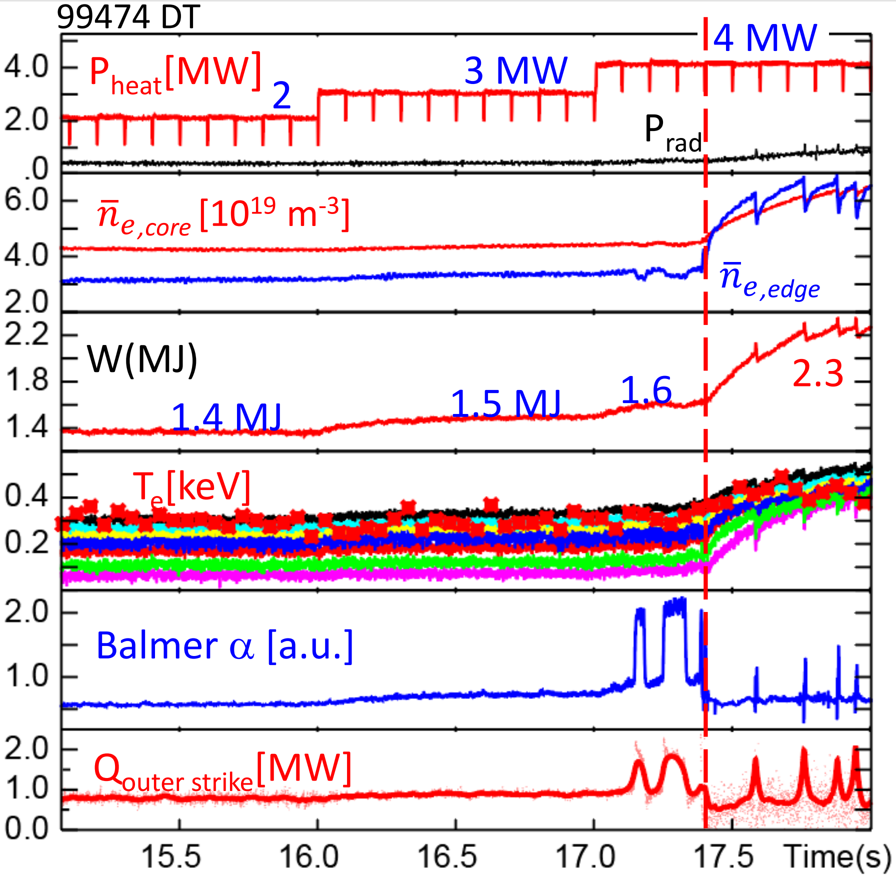

Experiment with constant gas

In L-mode

2 MW NBI:	1.4 MJ
3 MW NBI:	1.5 MJ
4 MW NBI:	1.6 MJ
L-H transition:	1.66 MJ

H-mode:

4 MW NBI:	2.3 MJ

…

L-H transition allows the plasma to keep heat and particles in

L-H transition: from Low to High confinement (H-mode)

JET 99474 DT (2021)

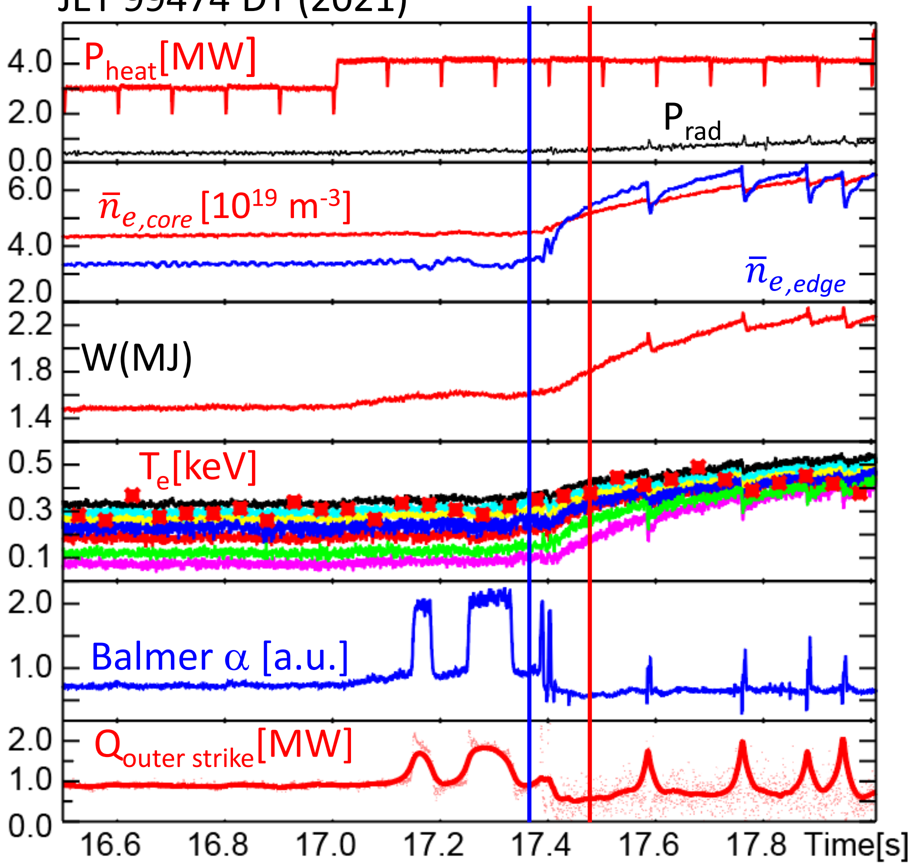

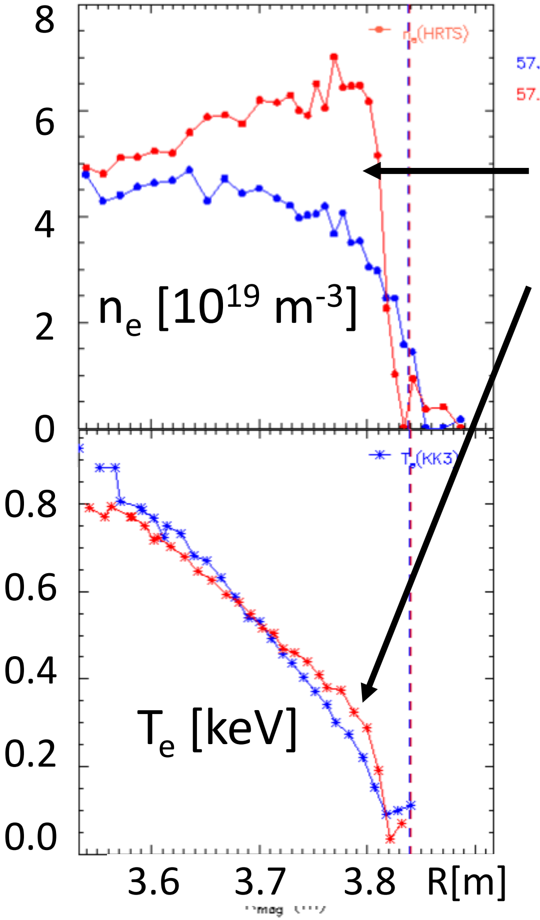

Pedestal formation

JET 3T, 2.5 MA: $\bar{n}_{e,min}$, $P_{LH,min}$, high and low ne branches

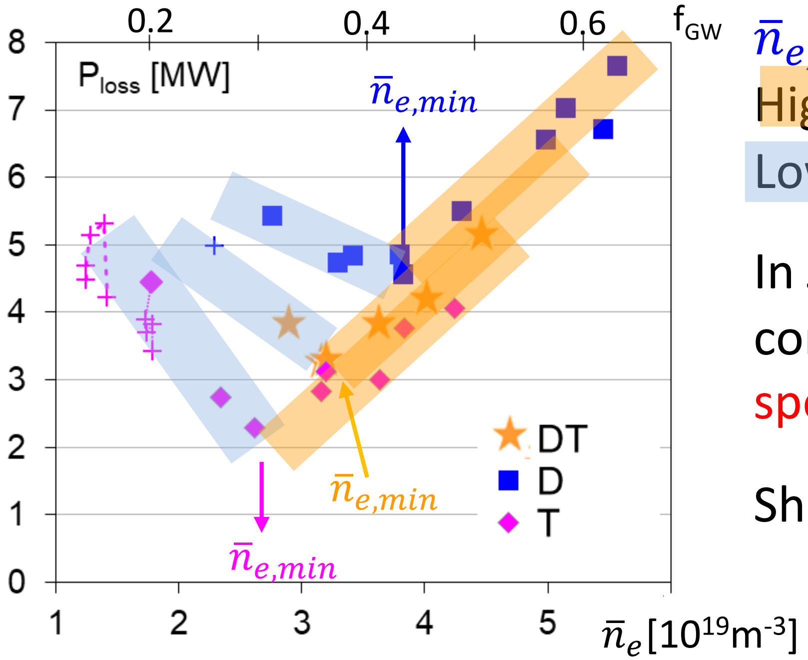

$\bar{n}_{e,min}$ is density at which P_{LH} is lowest, $P_{LH,min}$

High density branch: $\bar{n}_e > \bar{n}_{e,min}$

Low density branch: $\bar{n}_e < \bar{n}_{e,min}$

In JET $\bar{n}_{e,min}$ depends on plasma and divertor configuration/shape, divertor material, plasma species and plasma current.

Shift of $\bar{n}_{e,min}$ with isotope clearest in JET

Clear shift of $\bar{n}_{e,min}$: lowest for **T**, then **DT**, then **D**.

E.R. Solano et al., Nucl. Fusion ***63*** *(2023) 112011*

https://doi.org/10.1088/1741-4326/acee12

P_{LH} in 3T 2.5 MA dataset

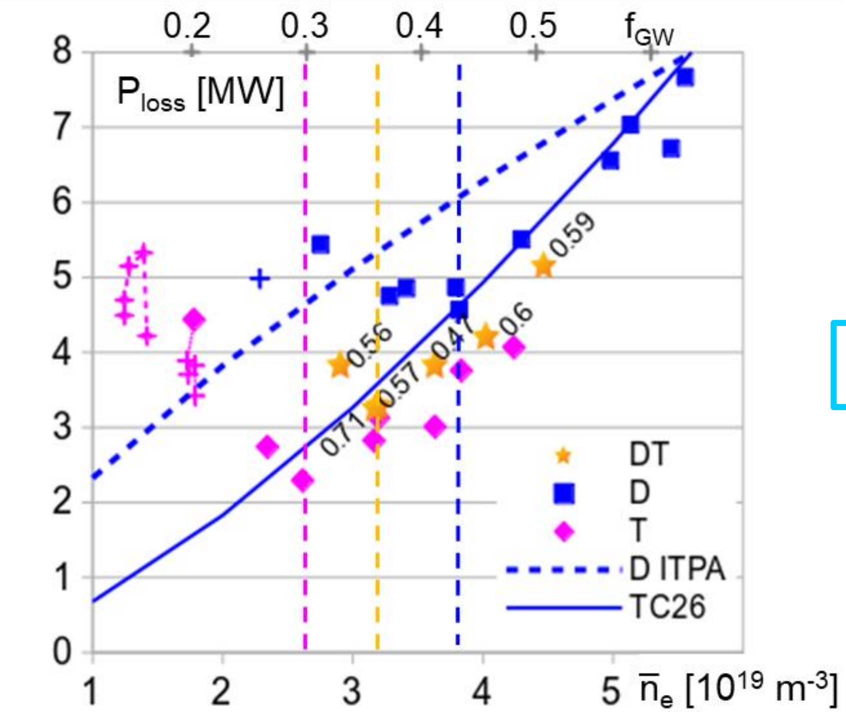

Potential easier access to H-mode in T-rich plasmas at lower density, to be evaluated *vs.* T consumption for ITER, DEMO, SPARC?

ITPA 2008 scaling doesn’t match D data

$$P_{ITPA}=0.049\, n_{e20}^{\mathbf{0.72\pm0.03}}\, B_T^{0.83\pm0.03}\, S^{0.94\pm0.02}(2/A)$$

New JET scaling proposed, stronger dependency on n_e

$$P_{TC26\text{-}iso} = 0.057\, \bar{n}_{e20}^{1.43}\, B_{tor}^{0.77}\, S\, (2/A_{eff})$$

Work ongoing:

multimachine metal P_{LH} scaling, including new JET data (E Delabie, APS 2024)

Critical profiles at L-H transition

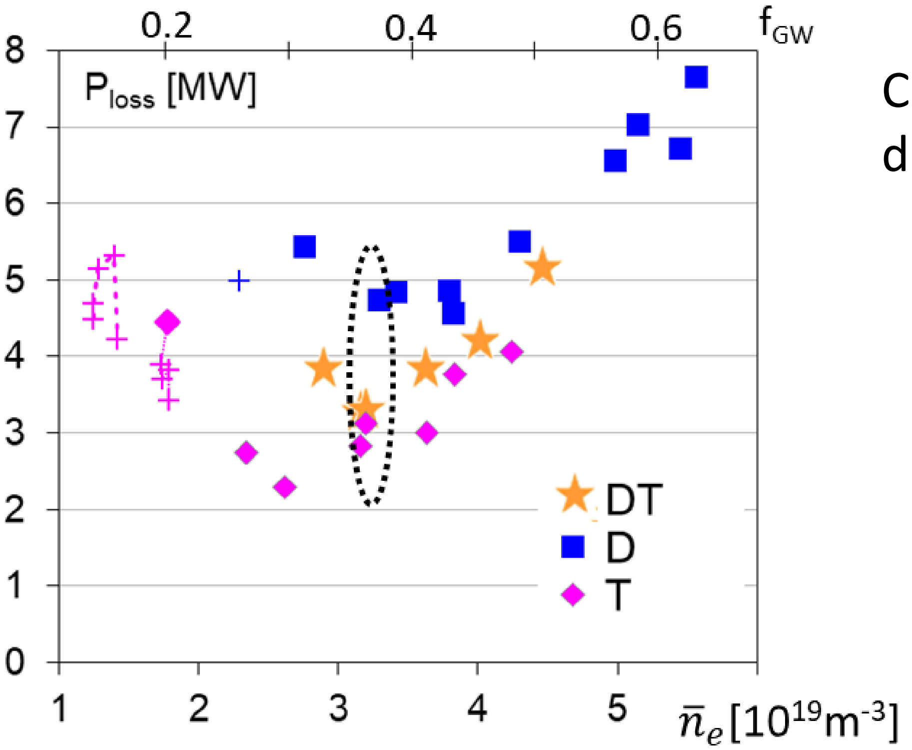

Compare profiles at transition for different species, at given density

E.R. Solano et al., Nucl. Fusion ***63*** *(2023) 112011*

3T 2.5 MA critical profiles

Thomson Scattering < 50 ms before L-H

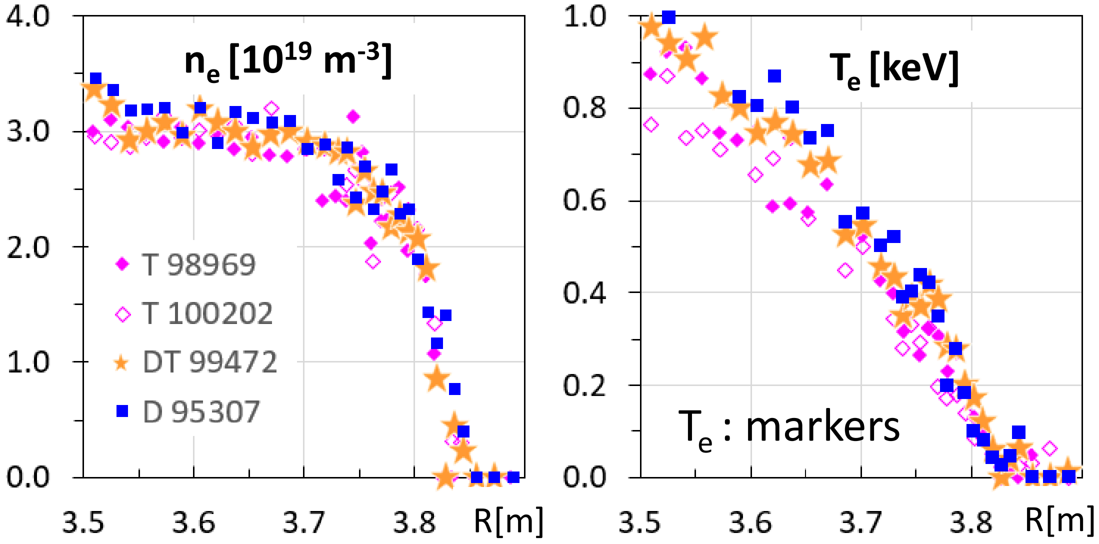

From r/a=0.5, very similar n_e, T_e, T_i profiles just before the transition in D, DT ,T

ER Solano IAEA FEC 2023

3T 2.5 MA critical profiles

Thomson Scattering < 50 ms before L-H

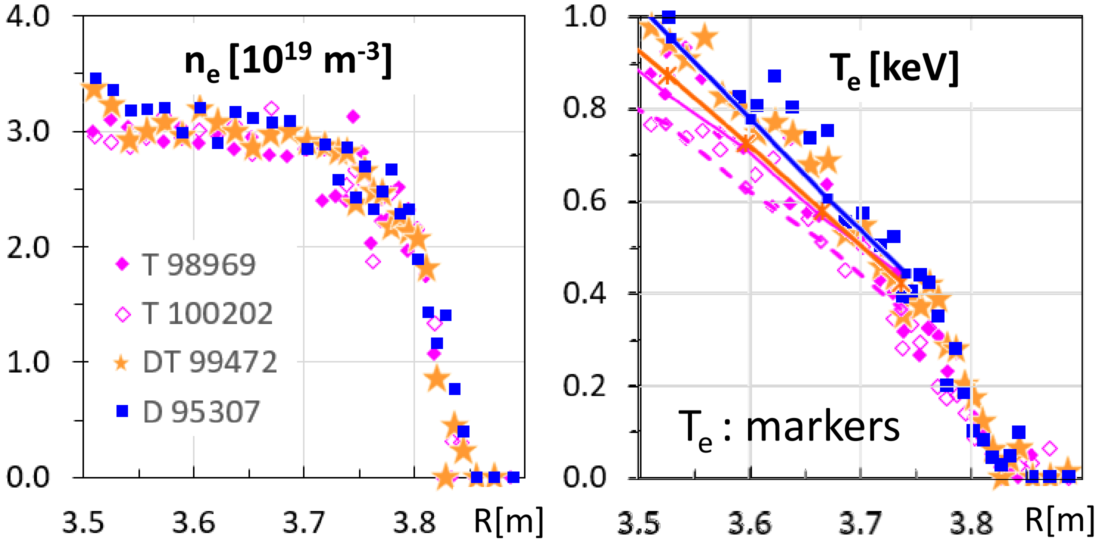

T_i~T_e (solid lines), Core CX

From r/a=0.5, very similar n_e, T_e, T_i profiles just before the transition in **D**, **DT** ,**T**

ER Solano IAEA FEC 2023

3T 2.5 MA critical profiles

Thomson Scattering < 50 ms before L-H

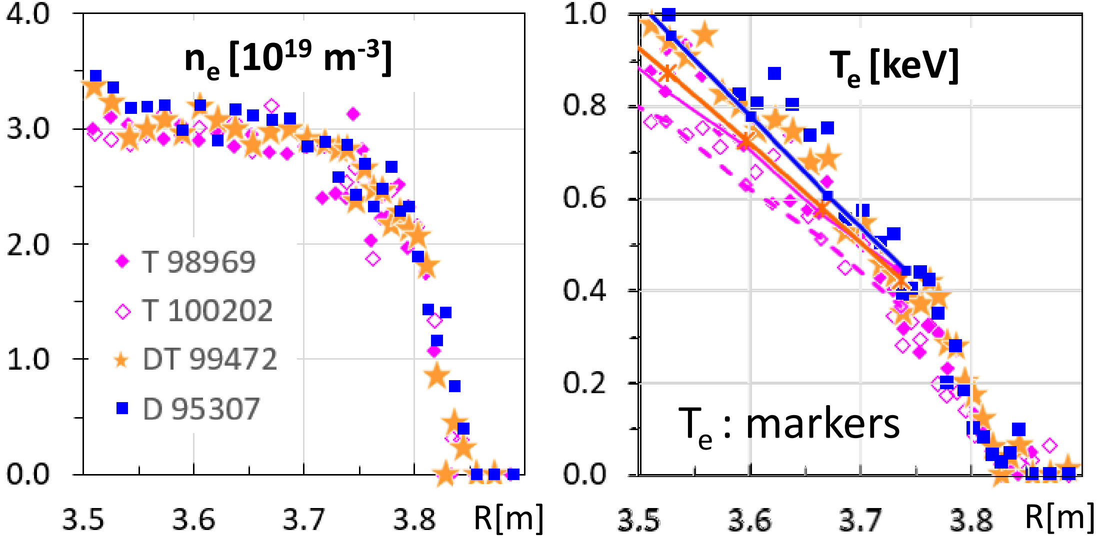

Same profiles at transition require very different P_{LH} depending on plasma isotope:

T : 3 MW
DT: 3.2 MW
D : 5 MW

Isotope effect on transition rooted on isotope effect in L-mode

Critical profiles for varying H+T mixtures (1.8T 1.7 MA)

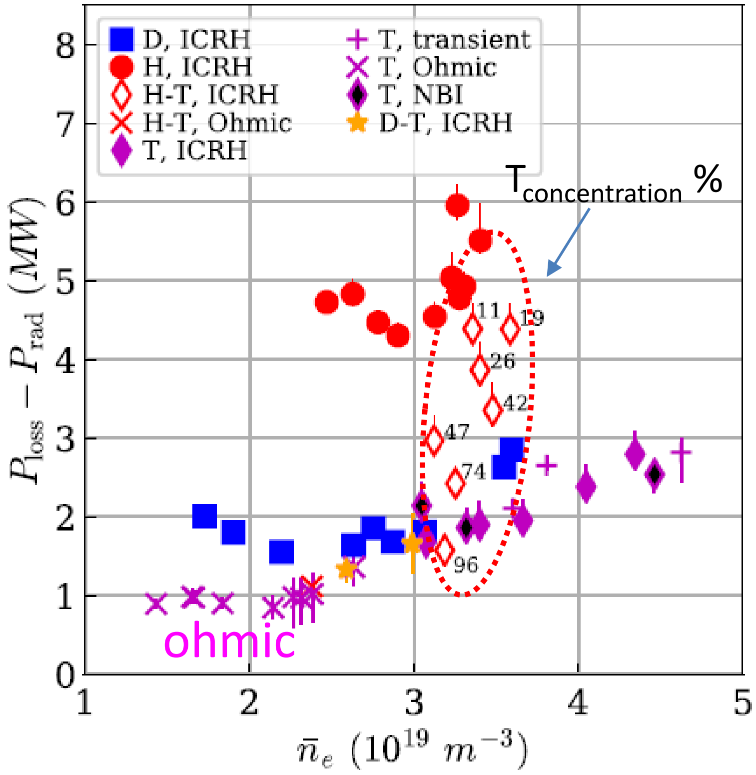

$T_{concentration}$ ⇧

P_{sep} ⇩

Hydrogen has much higher P_{LH} than Deuterium, larger than Tritium

Critical profiles for varying H+T mixtures (1.8T 1.7 MA)

G. Birkenmeier et al., PPCF (2023)

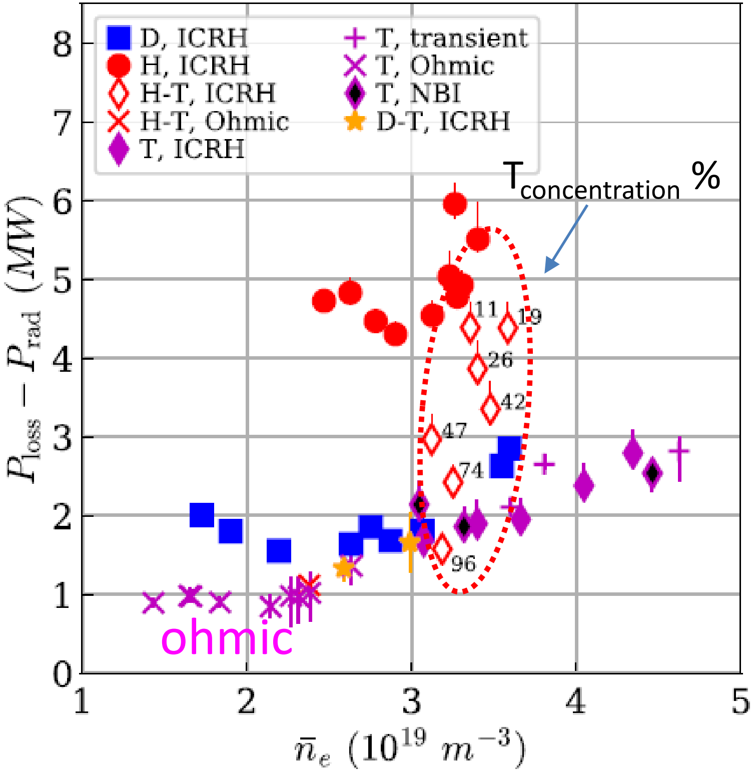

Isotopic dependency of L-mode transport defines P_{LH}

$T_{concentration}$ ⇧

P_{sep} ⇩

Same critical profiles for all mixtures

Critical profiles? Or critical ∇p_e, ∇p_i or ∇p_{total}?

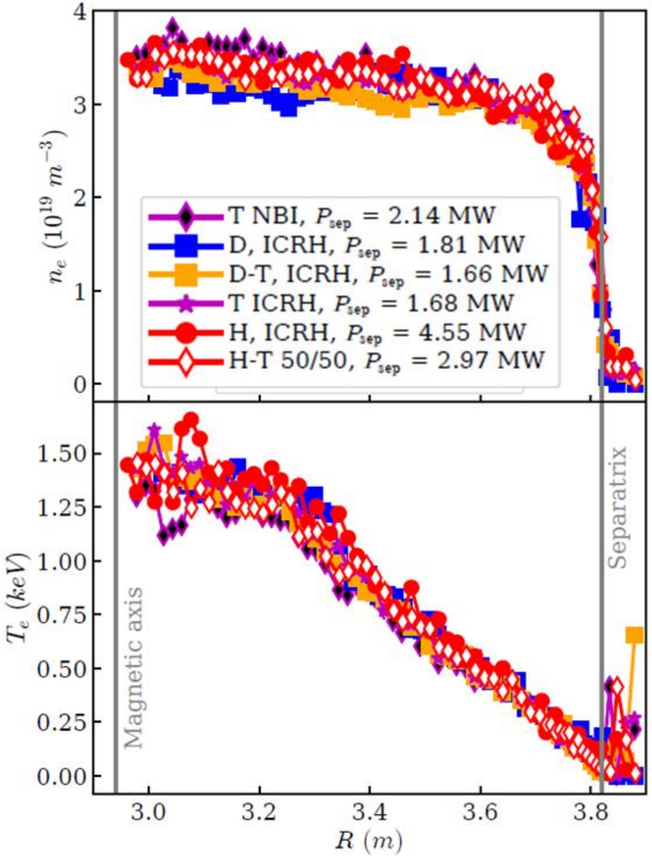

Critical profiles for varying H+T mixtures

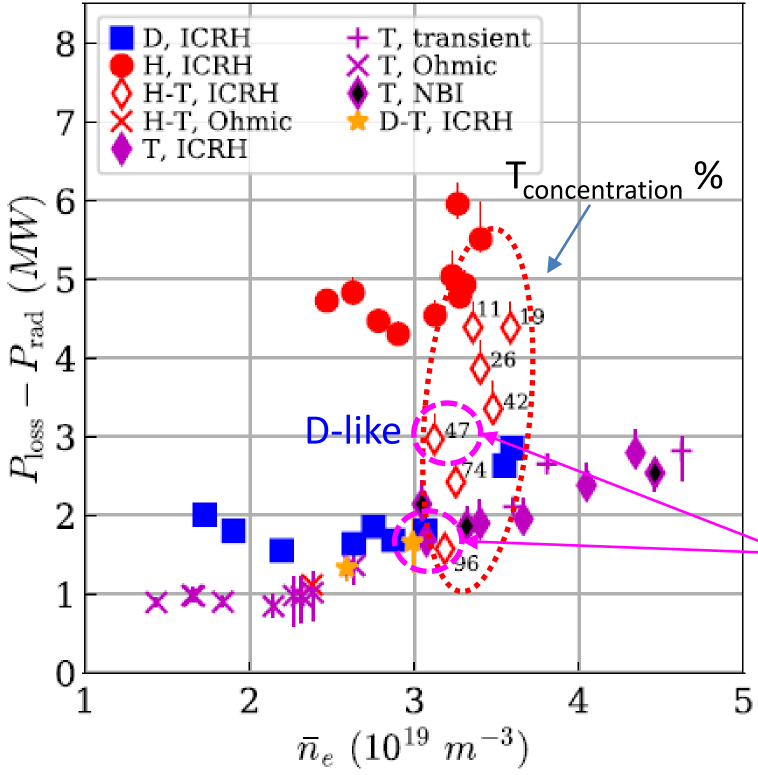

$T_{concentration}$ ⇧

P_{sep} ⇩

Same critical profiles for all mixtures

A_{eff} not good!

Critical profiles? Or critical ∇p_e, ∇p_i or ∇p_{total}?

G. Birkenmeier et al., PPCF (2023)

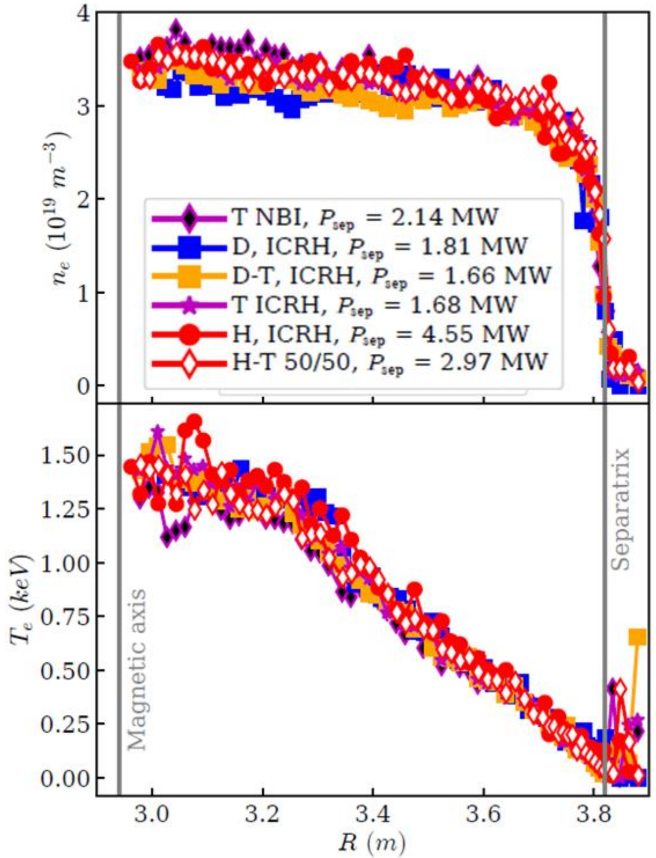

Isotopic dependency of L-mode transport defines P_{LH}

Theory?

Why does the L-H transition happen?

- In L-mode: turbulence is strong
- In H-mode: turbulence reduced
- The ExB model/paradigm

  Sheared ExB rotation breaks up turbulent eddies, reduces turbulent transport
- **Known**: H-mode profiles stabilise turbulence, L-mode profiles don't
- **But L-H transition trigger remains unknown**

Multiple theories develop ExB idea, based on electrostatic turbulence

None succeed in simulating **transition** *consistent with measurements*

Contour plots of turbulence amplitude, $\frac{e\tilde{\Phi}}{T}$ (simulation)

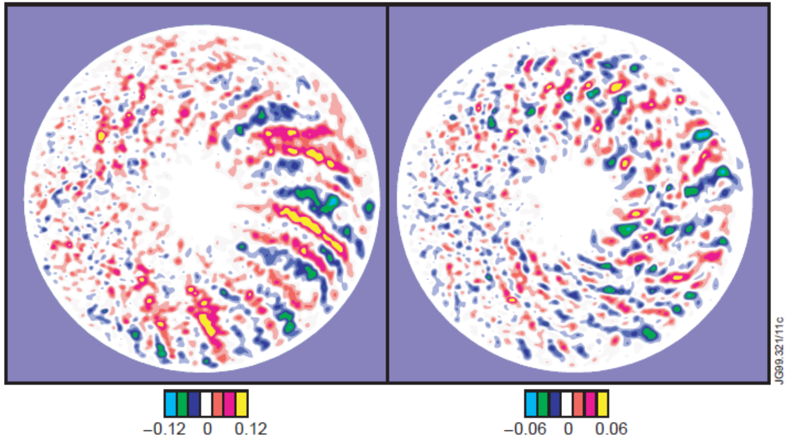

Without Sheared Flow *With* Sheared Flow

Z. Lin, Science 281,1835(1998)

Experimental counter-evidence in Deuterium at JET: Doppler reflectometry measurement of $v_\perp$

Typical results of $P_{L\text{-}H}$ density scan in Deuterium

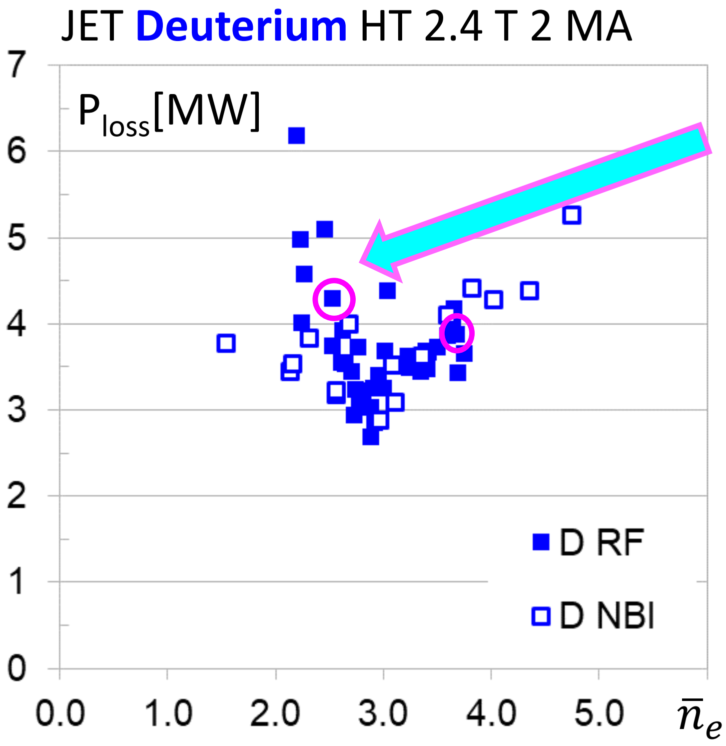

Focus on L-H transition with very detailed Doppler reflectometry measurements

Doppler reflectometry measures $v_\perp$, rotation of fluctuations perpendicular to B

$v_\perp$ shear is exactly what will tear or stretch turbulence eddies', if that is the mechanism for L-H transition

$v_\perp \sim ExB/B^2$ (different from v_{ion})

Doppler reflectometry along power ramp in Deuterium

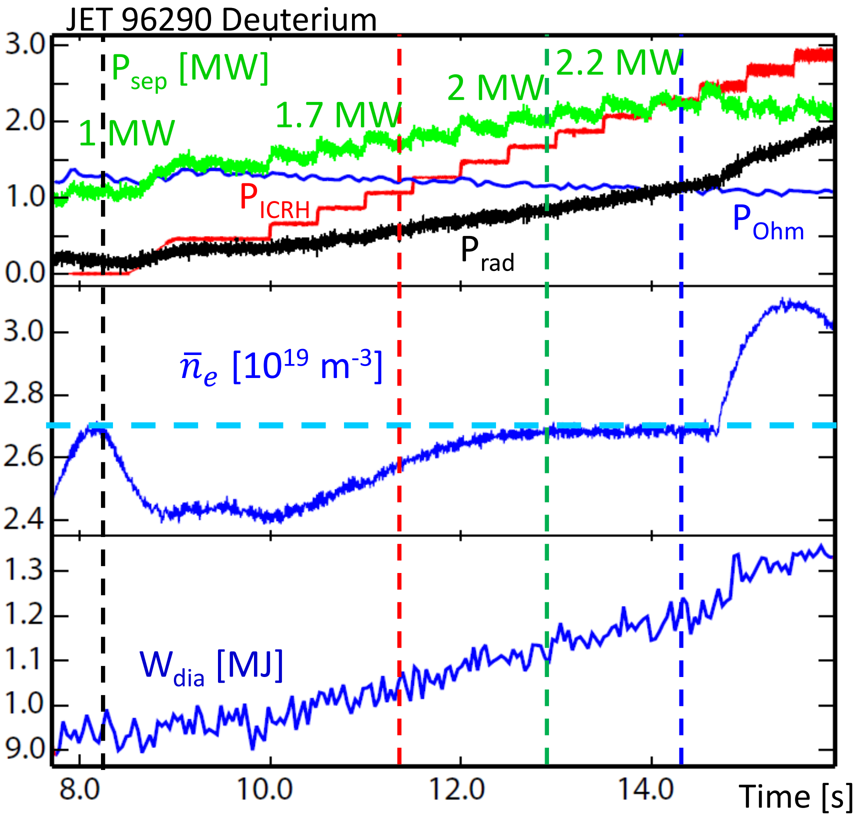

C. Silva, Nucl. Fus. 61 126006 (2021)

Doppler reflectometry along power ramp in Deuterium

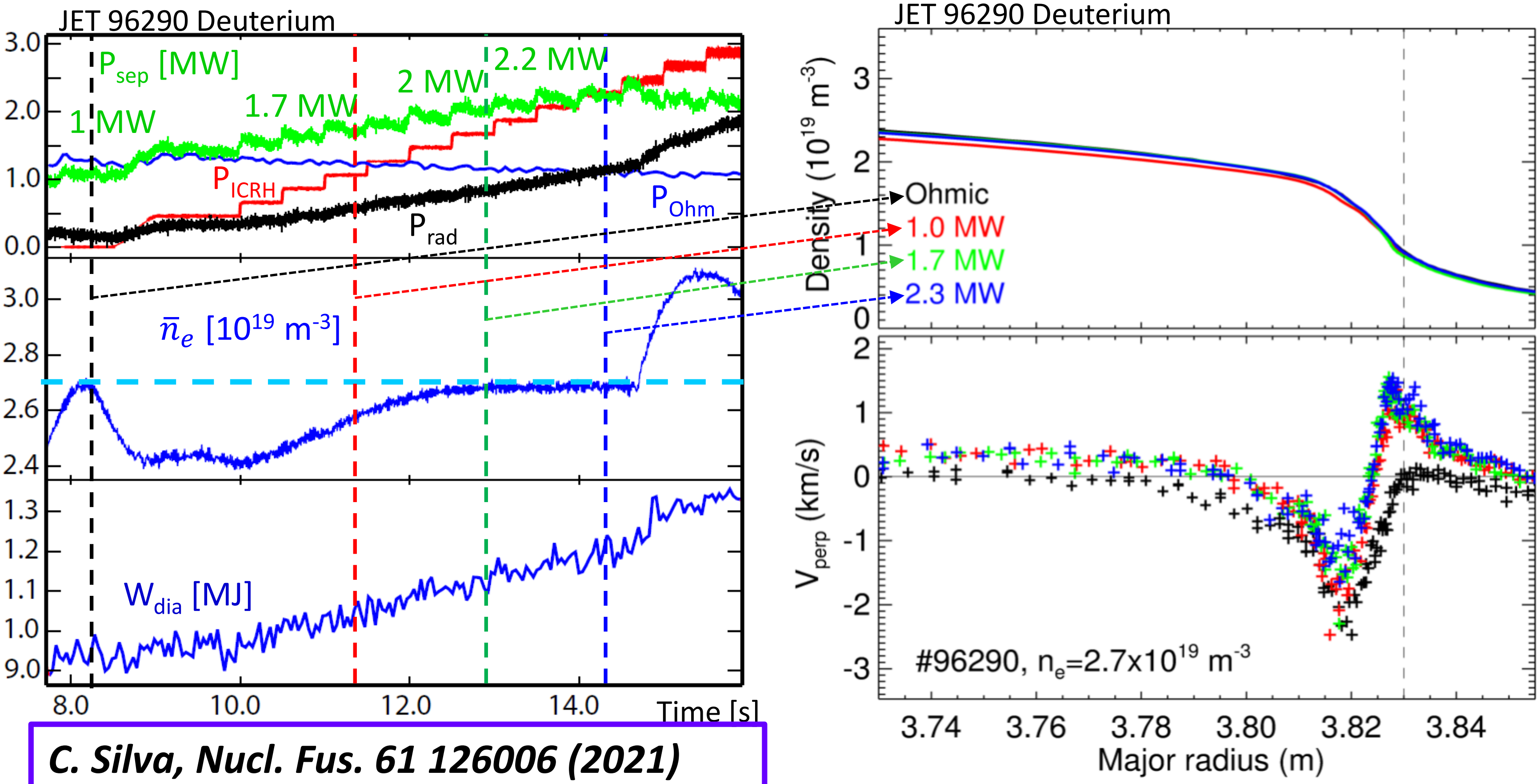

C. Silva, Nucl. Fus. 61 126006 (2021)

Deuterium: E_r measurements along ICRH power ramp, at $n_{e,min}$(D)

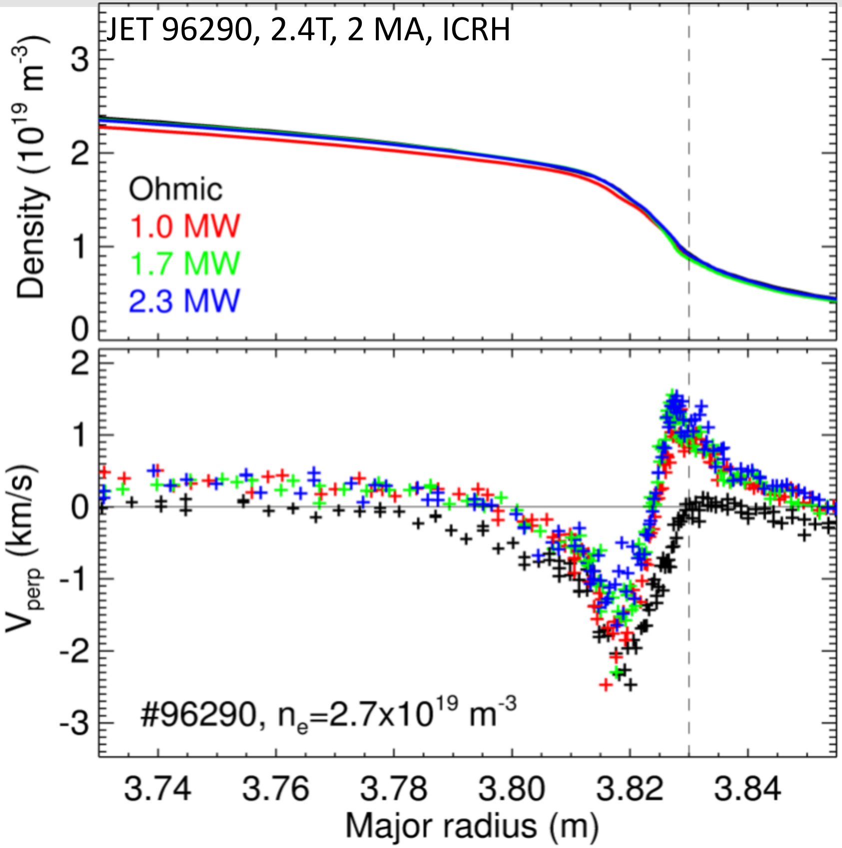

C. Silva, Nucl. Fus. 61 126006 (2021)

Time resolution: 300 ms (~τ_E)

No momentum input, RF heating

Ohmic: low $v_\perp$ at separatrix/SOL, deep well

During power ramp:

- high $v_\perp$ at separatrix/SOL when ICRH on
- reduction in depth of $v_\perp$ well with ICRH
- similar $v_\perp$ maximum shear during power ramp

$$\vec{v}_\perp = \frac{\vec{E}\times\vec{B}}{B^2} \sim Er/B$$

Neither $v_\perp$ well nor $v_\perp$ shear increase during the power ramp. No critical E_r well depth

Is this $v_\perp$ shape characteristic of L-mode?

If so, what triggers the L-H transition?

T_e profile does evolve along the power ramp

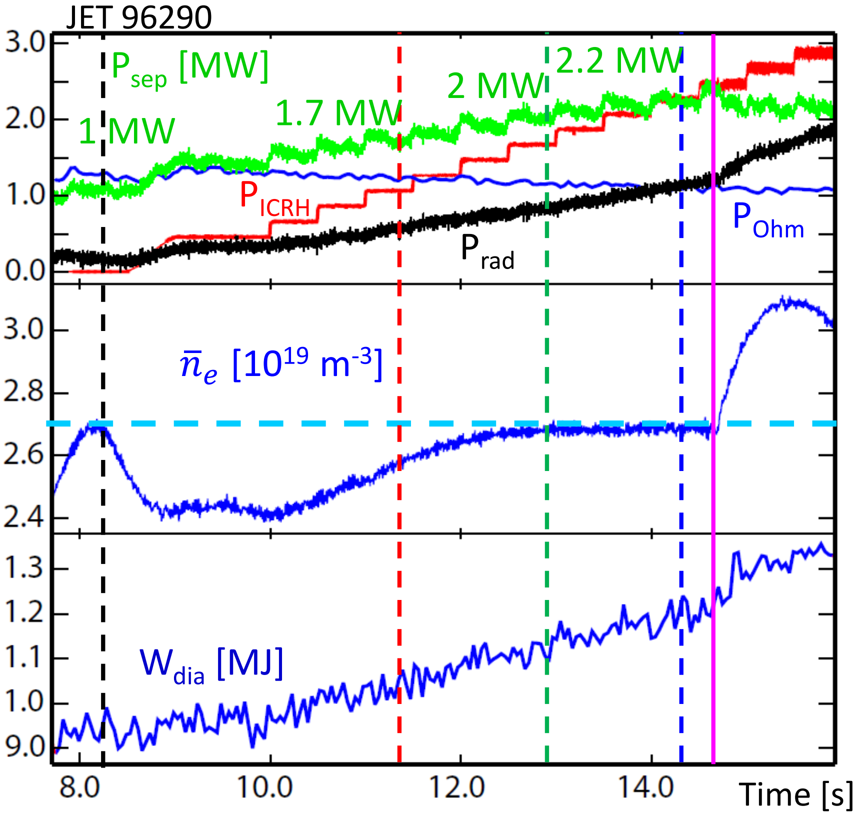

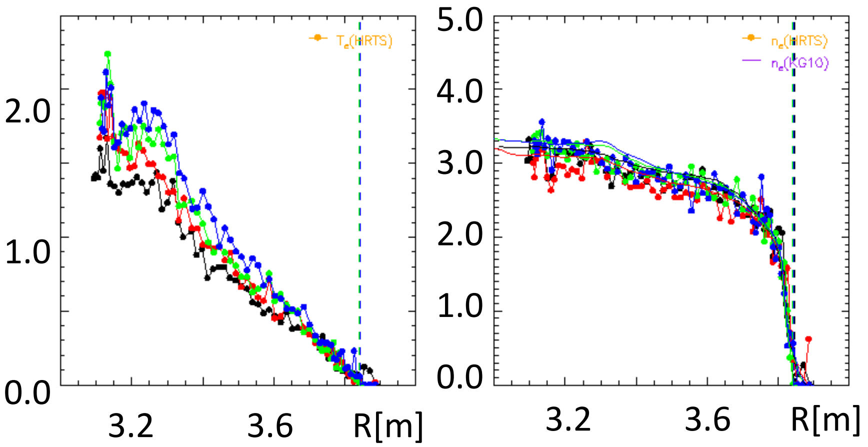

- Plasma heated with Ion Cyclotron RF: no T_i or rotation measurements available.

- ∇p does steepen along power ramp.
- Critical ∇p or ∇p_e or ∇p_i ? Not critical E_r.

JET L-H experimental results

- Critical profiles n_e, T_e, T_i determine access to L-H transition
- P_{LH} depends on isotope due to L-mode isotopic dependencies
  - L-mode τ_E scaling is VERY old (1989), needs revisiting, especially isotope effect
- Effective mass orders threshold, but not good scaling parameter
- $v_\perp$ profile doesn't evolve along power ramp

And what about theory?

Magnetization phase transitions: explored in
Equilibrium criticality when $j_\theta=0$: ER Solano, PPCF 46 L7 (2004)
Diamagnetism and ITB formation: J Garcia, G Giruzzi PRL 104 205003 (2010)
Magnetic phase transition, transport barriers: ER Solano & RD Hazeltine NF 52 114017 (2012)

Plasma magnetization in a tokamak

Plasma force balance: $\nabla p = \vec{j} \times \vec{B} = \vec{j}_\zeta \times \vec{B}_\theta + \vec{j}_\theta \times \vec{B}_\zeta$

In cylindrical approximation $\frac{d}{dr}\left(p + \frac{B_z^2 + B_\theta^2}{2\mu_0}\right) = -\frac{B_\theta^2}{r\mu_0}$

$$\boxed{\frac{dB_z}{dr} = -\mu_0 j_\theta}$$

Integrating:

$$\beta_\theta \equiv \frac{\int_0^a p dS}{B_{\theta a}^2 / 2\mu_0} = \frac{B_{za}^2 - \langle B_z^2 \rangle}{B_{\theta a}^2} \simeq 1 + \frac{2B_{za}\left(B_{za} - \langle B_z \rangle\right)}{B_{\theta a}^2}$$

β_θ related to volume averaged plasma magnetization

$\beta_\theta < 1$

$\nabla p < j_z \times B_\theta$

B_z increased by j_θ, paramagnetism, low pressure

$\beta_\theta > 1$

$\nabla p > j_z \times B_\theta$

B_z reduced by j_θ diamagnetism, high pressure

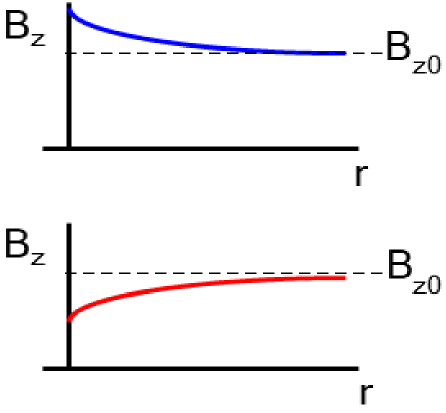

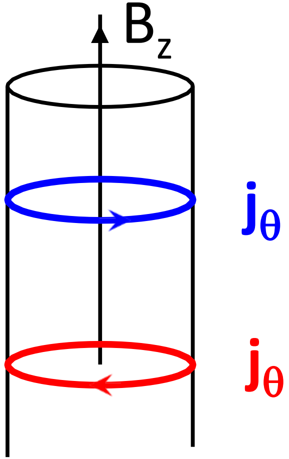

Plasma Magnetisation

The tokamak plasma is a magnet

Sign of j_θ describes local magnetisation

Magnetisation phase boundary at $j_\theta=0$

Paramagnets

increase the background magnetic field

move towards high field

Diamagnets

increase the background magnetic field

move towards low field

Diamagnetic frog levitating in magnetic field
Berry, Geim (Ig-Nobel)
Eur. J. Phys. **18** 307 1997

Magnetism in cylindrical blob with pressure peak/hole

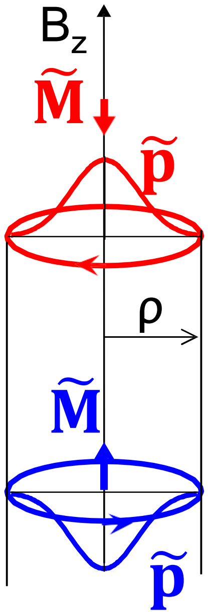

$$\mathbf{F} = mn\frac{d\mathbf{v}}{dt} = -\nabla\tilde{p} + \tilde{\mathbf{j}}\times\mathbf{B} = 0 \qquad \tilde{\mathbf{j}}_\perp = \frac{\mathbf{b}\times\nabla\tilde{p}}{B}$$

Diamagnetic current: if inside the tube there is a pressure peak, the associated $j_\perp$ reduces B_z: diamagnetism

Paramagnetic current: if inside the tube there is a pressure hole, the associated $j_\perp$ increases B_z: paramagnetism

Magnetization of the blob:

$$\nabla\times\mathbf{M} = \mu_0\frac{b\times\nabla\tilde{p}}{B} = -\frac{dM}{dr}\hat{\mathbf{r}}$$

$$\tilde{\mathbf{M}} = \frac{1}{\lambda_\parallel}\int_0^{\rho}\frac{\mathbf{b}}{B}\frac{\partial\tilde{p}(\rho')}{\partial\rho'}\lambda_\parallel\, d\rho' \approx -\frac{\tilde{p}}{B}\mathbf{b} \quad \begin{cases} < 0, \text{ dia} \\ > 0, \text{ para} \end{cases}$$

Movement of magnetised blobs in paramagnetic plasma

Jackson, Classical Electrodynamics

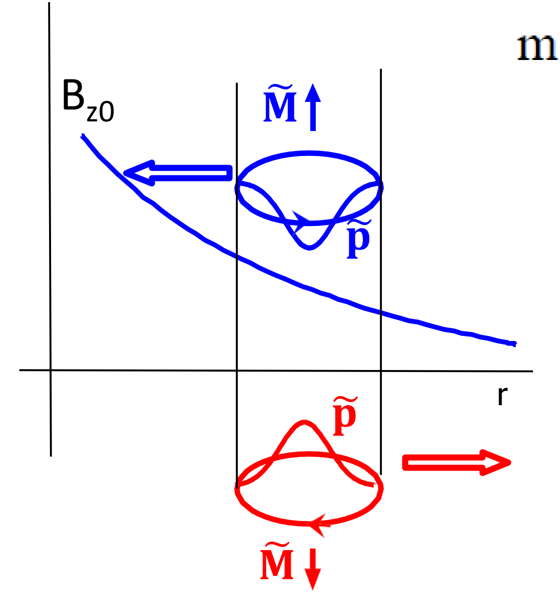

$$m_V \frac{d\mathbf{v}}{dt}\bigg|_V = \int \left(\nabla(\tilde{\mathbf{M}}.\mathbf{B})\right) dV \simeq \left(\int (r \times j_{mag}) dV\right) \int \nabla B_{0z} dV$$

blob magnetization

$$\boxed{\vec{B} = \vec{B}_0 + \vec{r}.\nabla\vec{B}_0 + \ldots}$$

$$mn_V \frac{d\mathbf{v}_r}{dt} \simeq \tilde{M}_z \nabla \bar{B}_{z0}$$

the cold blob (paramagnetic) seeks high field

the hot blob tube (diamagnetic) seeks low field

Blob averaged dB_z/dr controls motion of magnetised plasma

blobs: <u>Anti-potential</u> leads to *magnetic phase separation*

Paramagnetic plasma: L-mode

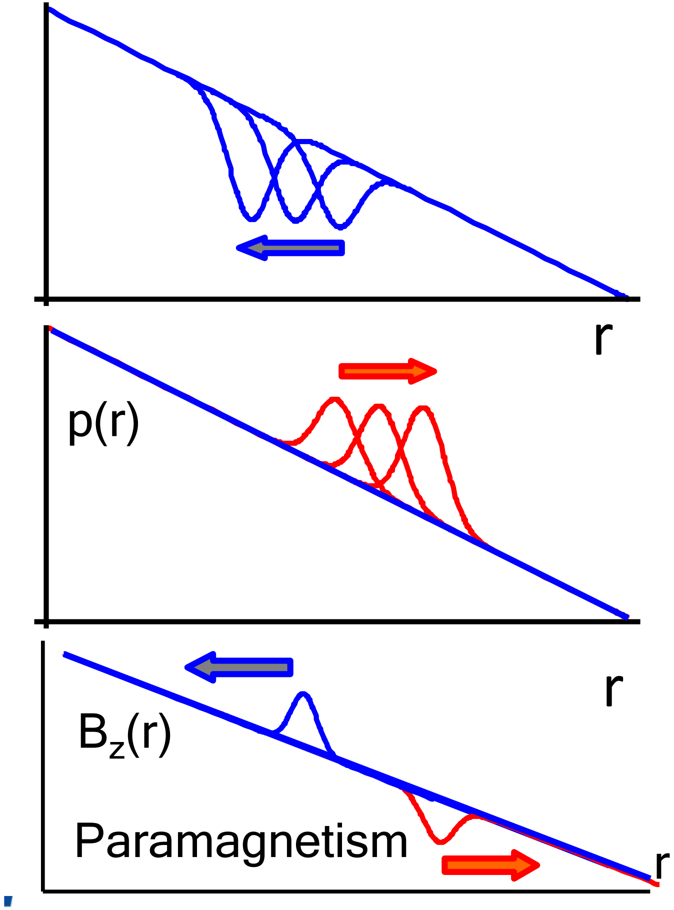

Motion of pressure blobs depends on dB_z/dr

$$mn_V \frac{d\vec{v}_r}{dt} \simeq \tilde{M}_\zeta \nabla_r \bar{B}_{\zeta 0}$$

paramagnetic cold blobs move inward,

diamagnetic hot blobs move outward

outward thermal energy convection at the expense of

inward magnetic energy convection

p blobs “grow”, “instability”

L-mode

Diamagnetic plasma: H-mode

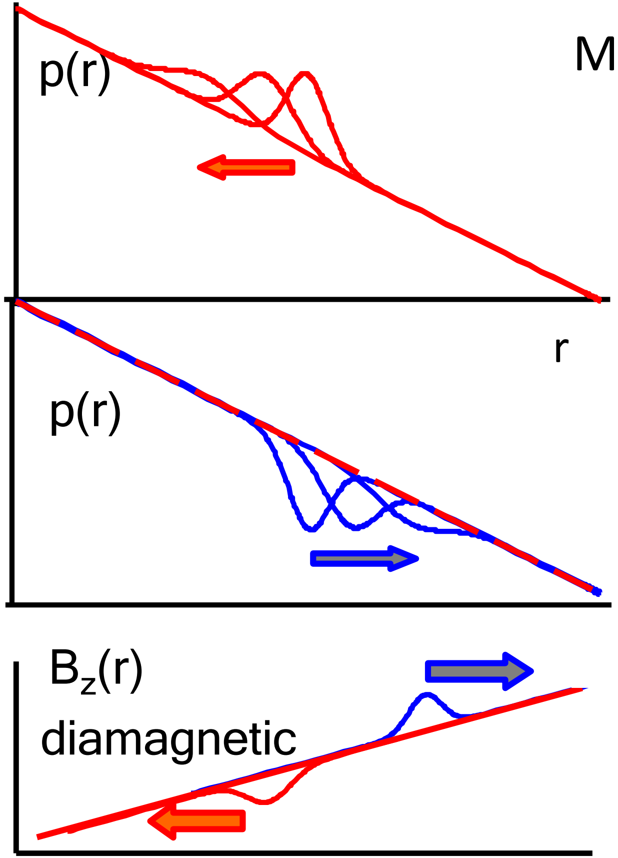

Motion of pressure blobs depends on dB_z/dr

$$mn_V \frac{d\vec{v}_r}{dt} \simeq \tilde{M}_\zeta \nabla_r \overline{B}_{\zeta 0}$$

diamagnetic hot blobs move inward,

paramagnetic cold blobs move outward

inward thermal energy convection

at the expense of

outward magnetic energy convection

p blobs “decrease”, “saturation”

H-mode

Magnetic Boundary: phase transition

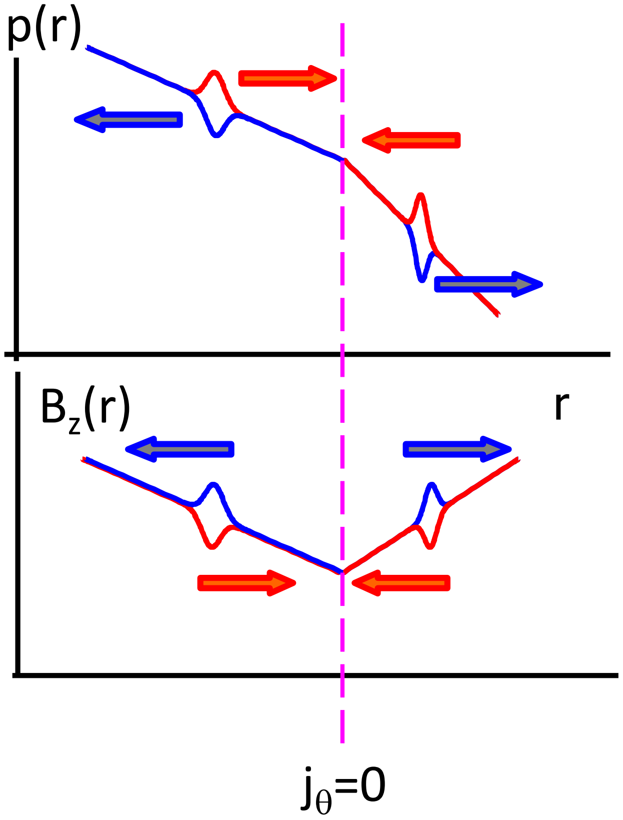

At a magnetic phase boundary blobs of the
same type accumulate/separate

diamagnetic blobs (heat) seek magnetic wells
paramagnetic blobs seek magnetic hills

With multiple blobs moving,
p and B_z profiles evolve,
steepening magnetic hills, digging magnetic wells
Developing pressure pedestal

Pedestal formation at magnetisation boundary

Assume dashed $B_z(r)$, $p(r)$ initial profiles

Ideal MHD with magnetization force

$$\bar{n}_V m_i \frac{d^2\xi_r}{dt^2}\Big|_M = \tilde{M}_\zeta \nabla \bar{B}_{0z}$$

$$\frac{\partial B_z}{\partial t}\Big|_M = \nabla\times(\tilde{v}_r \bar{B}_{0z})$$

$$\frac{3}{2}\frac{\partial p}{\partial t}\Big|_M = -\nabla(\tilde{p}\,\vec{v})$$

Integrating one temporal step

pressure steepens in diamagnetic regions, increases diamagnetism
flattens in paramagnetic regions, increases paramagnetism

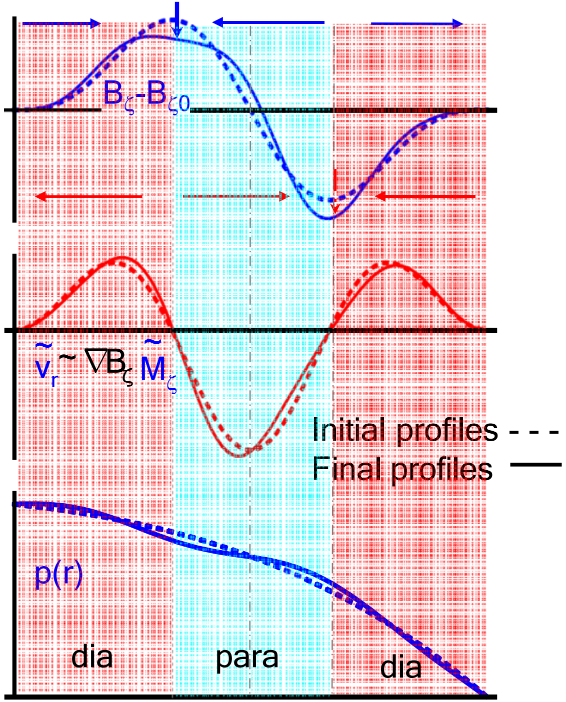

Magnetic phase separation drives pedestal formation

Interchange instability[1]

- present when radial force acts equally on electrons and ions
- equivalent to the Rayleigh-Taylor instability in a fluid.
- magnetization gradient acting on magnetized plasma blobs replace "gravitational field" or "curvature".

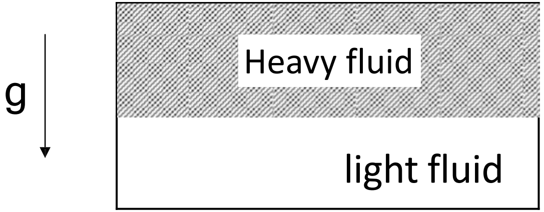

Magnetization interchange

$$\gamma = \sqrt{g\lambda_\perp} =$$

$$= \sqrt{-\frac{1}{m_V}\frac{\tilde{p}}{2B^2}\frac{\partial B_\zeta^2}{\partial r}\lambda_\rho}$$

Magnetization interchange growth faster for
high magnetisation, blob amplitude & radius, low field & mass

[1] M.N. Rosenbluth and C.L. Longmire, Annals of Physics, Volume 1, Issue 2, May 1957,120

Suydam criterion for interchange instability

B. R. Suydam, Proc. 2nd UN Conf. on Peaceful Uses of Atomic Energy, Geneva, 1958.

$$\beta'\left(\frac{Rq}{r_s}\right)^2\left[\frac{B^2\kappa_r}{\mu_0}\right] > \frac{q'^2}{4q^2}$$

magnetic shear opposes interchange of tubes driven by cylindrical curvature and $\nabla\beta$

Generalization: add magnetization force to cylindrical curvature

$$\beta'\left(\frac{Rq}{r_s}\right)^2\left[\frac{B^2\kappa_r}{\mu_0} + \tilde{M}_z\frac{dB_{0z}}{dr}\right] > \frac{q'^2}{4q^2}$$

In magnetically mixed states $\tilde{M}_z\frac{dB_{0z}}{dr} < 0$

magnetisation force adds to curvature, instability,

until the magnetic shear q’ or the sign of dB_z/dr changes.

L-H transition power threshold

JET Petition

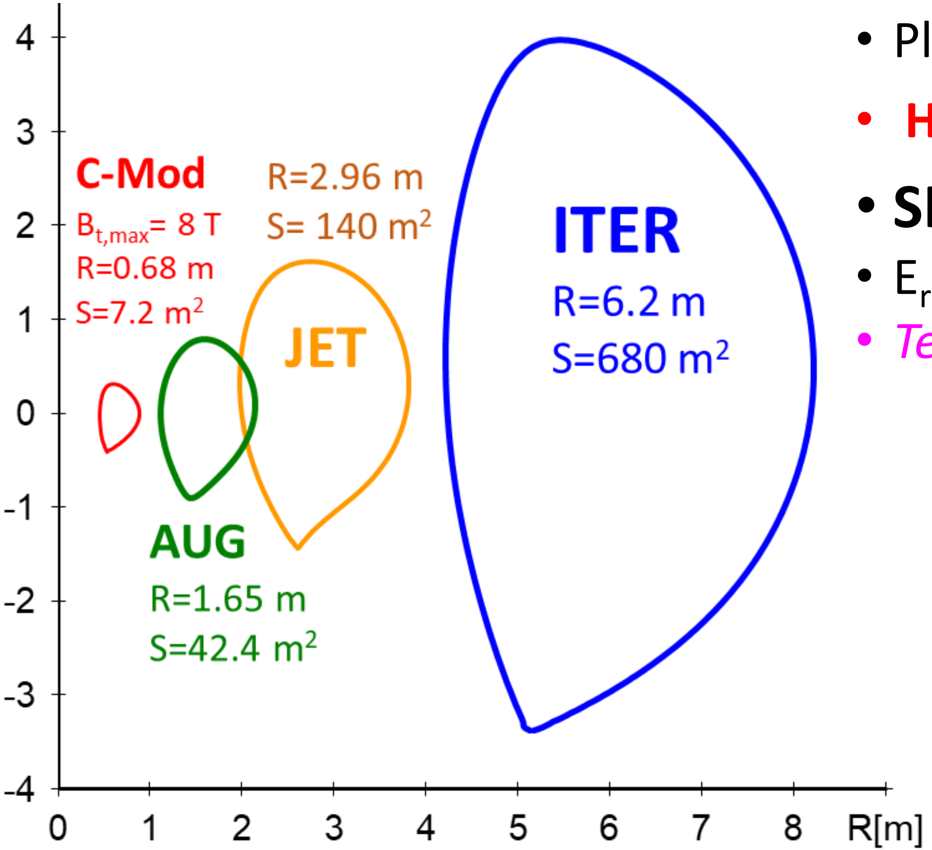

- Plasma shape affects P_{LH}
- **H**, **D**, **DT**, **T** affects P_{LH}
- **SIZE** and **current** matters
- E_r shear not the only ingredient?
- *Test magnetisation phase transition model?*

Conventional L-H models unlikely to explain our detailed measurements

Much work yet to be done

at JET?